Inorganic Chemistry

Article

pubs.acs.org/IC

Theoretical Prediction of Spin-Crossover Temperatures in Ligand-Driven Light-Induced Spin Change Systems

Jordi Cirera and Francesco Paesani*

Department of Chemistry and Biochemistry, University of California, San Diego, 9500 Gilman Drive, La Jolla, California 92093-0314, United States

Supporting Information

ABSTRACT: Spin-crossover compounds exhibit two alternative spin states with distinctive chemical and physical properties, a particular feature that makes them promising materials for nanotechnological applications as memory or display devices. A key parameter that characterizes these compounds is the spin-crossover temperature, $T_{1/2}$, defined as the temperature with equal populations of high and low-spin species. In this study, a theoretical/computational approach is described for the calculation of $T_{1/2}$ for the *trans*-[Fe(styrylpyridine)$_4$(NCX)$_2$] (X = S, Se, and BH$_3$, styrylpyridine in the *trans* configuration) ligand driven light-induced spin change (LD-LISC) complexes. In all cases, the present calculations provide an accurate description of both structural and electronic properties of the LD-LISC complexes and, importantly, predict spin-crossover temperatures in good agreement with the corresponding experimental data. Fundamental insights into the dependence of $T_{1/2}$ on the nature of the axial ligands are obtained from the direct analysis of the underlying electronic structure in terms of the relevant molecular orbitals.

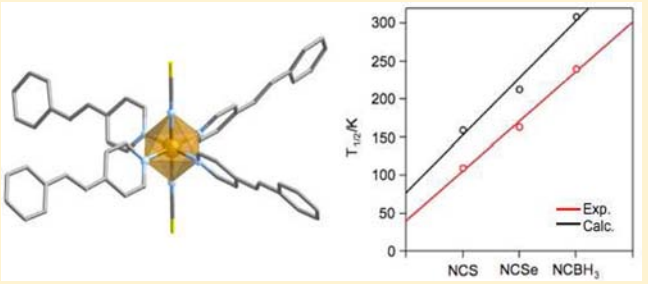

1. INTRODUCTION

Spin-crossover (SC) systems are transition metal compounds in which the metal center can adopt more than one spin state.[1−8] This peculiar property depends on several factors that include the coordination number and nature of the ligands as well as the specific electronic configuration of the metal center. Although there is a wide range of possible combinations of ligand fields and coordination numbers that can lead to the spin-crossover phenomenon, the octahedral coordination is most commonly found in the SC compounds. In this geometry, the d orbitals of the metal center split into the t_{2g} and e_g sets of orbitals, resulting in two possible spin states for metals with d^4−d^7 electron configuration. In weak ligand fields, the energy splitting is smaller than the electron-pairing energy, and the electrons are distributed over both the t_{2g} and e_g sets to give the maximum number of unpaired spin. As a result, the ground state of the complex is the high-spin (HS) state with maximum spin multiplicity. By contrast, in strong ligand fields the ground state of the complex is the low-spin (LS) state with the electrons pairing in the t_{2g} orbitals before filling up the e_g set. For intermediate situations, the energy difference between the lowest vibronic levels of the two spin states can be small enough that application of relatively minor external perturbations can induce a change in the spin state. This leads to the spin-crossover phenomenon that was first reported by Cambi and co-workers.[9] As a result of this behavior, spin-crossover systems are ideal prototypes for molecular switches which have attracted much interest for potential applications in molecular memory storage systems and nanoscale devices.[1,6,10−15]

Although thermally induced perturbations are most common, with the populations of the two spin states varying as a function of the temperature, pressure- and light-induced transitions have also been observed.[16−18] The latter can lead to the so-called light-induced excited spin state trapping (LIESST) effect in which the low-spin state is excited to a metastable high-spin state with a virtually infinite lifetime at low temperatures.[19−23] A new family of spin-crossover compounds containing photoreactive ligands has recently been reported in which the spin transition is induced by the interaction with the electromagnetic radiation.[24−27] In these systems, the organic ligands undergo a configurational change upon light adsorption, such as a *cis*/*trans* photoisomerization, which in turn modifies the ligand field strength and, consequently, induces the change of spin state on the metal ion. Among the ligand driven light-induced spin change (LD-LISC) systems, the family of [Fe(stpy)$_4$(NCX)$_2$] (stpy = 4-styrylpyridine; X = S, Se, BH$_3$, and BPh$_3$) complexes (Figure 1) is of particular interest. These compounds exhibit significantly different magnetic behavior depending on the specific configuration acquired by the stpy ligand. More specifically, it was found that, while the isomer with the stpy ligand in the *trans* configuration undergoes the spin crossover, the complex containing the *cis*-stpy isomer remains in the HS state at all temperatures. This was attributed to the decrease in the ligand field strength due to the equatorial ligand.[24−27] As shown in Figure 1, a key parameter for the

Received: April 12, 2012
Published: July 20, 2012

   dx.doi.org/10.1021/ic300750c | *Inorg. Chem.* 2012, 51, 8194−8201

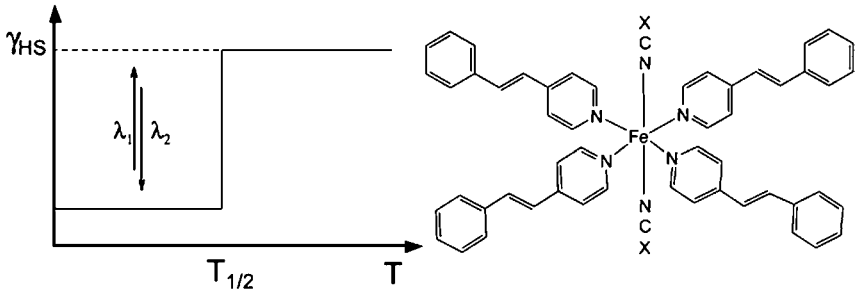

Figure 1. Schematic representation of the ligand-driven light-induced spin-crossover effect. Solid line for the complex incorporating the *trans*-stpy isomer, and dashed line for the complex incorporating the *cis*-stpy isomer. γ_{HS} is the relative population of the high-spin species, while λ_1 and λ_2 are the irradiating wavelengths used to trigger the *trans*/*cis* and *cis*/*trans* isomerization processes, respectively.

characterization of SC systems is the spin-crossover temperature ($T_{1/2}$) defined as the temperature with equal populations of the high- and low-spin states.[7,16] For actual technological applications, $T_{1/2}$ should lie within the room temperature range. In this regard, it has been shown that chemically different axial ligands can lead to significantly different values of $T_{1/2}$.[24−27] The interest in LD-LISC compounds increased in recent years because of their potential use as building blocks of metal−organic frameworks (MOFs).[28−34]

In silico modeling represents a powerful tool that can provide fundamental insights into the dependence of $T_{1/2}$ on the electronic structure and chemical properties of the LD-LISC complexes, which are not easily accessible by other means. Because of the relatively large size of these systems, density functional theory (DFT) is usually the method of choice for describing the underlying electronic structure.[35−39] Although it has been shown that several molecular properties can be well reproduced by DFT methods regardless of the functional (e.g., equilibrium geometries),[40,41] this is generally not the case for processes that involve qualitative changes in the electronic structure of the system. In particular, the change in the quantum numbers of the occupied orbitals is very sensitive to the specific description of the exchange (or Fermi) correlation within a given functional.[42] To overcome this limitation, several attempts have been made in recent years to develop new functionals capable of reproducing the correct ground state and electronic energy differences between spin states in SC systems.[43−48] Among the different functionals, the hybrid meta-GGA functional TPSSh[49,50] has been shown to predict with accuracy the enthalpy changes that are associated with then spin crossover in both iron and cobalt complexes.[51]

In this study, we present a DFT-based computational approach for the calculation of $T_{1/2}$ in the SC isomer of LD-LISC complexes. Through an extensive analysis of different functionals, we show that our approach is capable of reproducing in a quantitative way the spin-crossover behavior observed in these complexes. Importantly, the complete characterization of the underlying electronic structure in terms of the relevant molecular orbitals allows us to establish a direct correlation between the chemical properties of the axial ligands and the corresponding $T_{1/2}$ value of the complex. The article is organized as follows: In section 2, the computational methodology is described, while the results are discussed in section 3. The conclusions are then given in section 4.

2. METHODOLOGY

The theoretical modeling of the spin-crossover behavior in SC systems is very challenging due to the difficulties associated with the accurate calculation of the energy splitting between the low-spin and high-spin states.[52] Previous studies showed that pure DFT functionals generally tend to overstabilize the low-spin state.[53,54] By contrast, since the exact exchange stabilizes the states with higher multiplicities through the explicit inclusion of Fermi correlation,[55−58] hybrid functionals overstabilize the high-spin state.[36,43,44,47,48,51] Although density functionals specifically reparameterized to reproduce the experimentally measured energy splitting of particular compounds have been reported in the literature, these functionals appear not to be directly transferable to different SC systems.[59,60]

Among the different DFT methods, B3LYP(*),[45,47] which was derived from the original B3LYP functional adjusting the amount of Hartree−Fock exchange to 15%,[61] provides an accurate description of the magnetic properties of the $[Fe(N_H)S_4]L$ family (N_HS_4 = 2,2′-bis(2-mercaptophenylthio)diethylamino, L = CO, NO^+, PR_3, NH_3 and N_2H_4) of compounds.[47] The B3LYP(*) functional also predicts with accuracy the energy difference between the low- and high-spin states of the $[Fe(phen)_2(NCS)_2]$ complex, one of the most prominent members of the Fe(II) spin-crossover family.[45] The spin-state energy difference in Fe(II) compounds can also be determined with density functionals that combine the OPTX exchange functional[62] with the LYP[63] and PBE[64,65] correlation functionals. More recently, the meta-GGA hybrid TPSSh functional[50,66] has been used to investigate the magnetic properties of a relatively large group of spin-crossover complexes containing Fe(II) and Co(II).[51] In all cases, the calculated enthalpy differences are in good agreement with the available experimental data.[51] This suggests that the amount of Hartree−Fock exchange (10%) contained in the TPSSh functional is appropriate for a correct description of the exchange correlation in complexes containing first row transition metals. Double hybrid functionals have also been used in calculations of the spin-state energetics of different SC compounds. However, due to the associated computational costs, the application of these functionals is currently limited to relatively small systems.[67]

In this study, the OLYP,[62,63] OPBE,[62,64,65] B3LYP(*),[47] and TPSSh[50,66] functionals are used to calculate the electronic energy differences of *trans*-$[Fe(stpy)_4(NCX)_2]$ complexes with X = S, Se, and BH_3. Previous studies have shown that these functionals are capable of reproducing, at least to some degree, the electronic energy differences in several spin-crossover systems.[43,46−48,51] All DFT calculations were carried out with Gaussian 09 using a 10^{-8} convergence criterion for the density matrix elements.[68] The fully optimized contracted triple-ζ all electron Gaussian basis set developed by Ahlrichs and co-workers was employed for all the elements with polarization functions being added on the Fe center.[69]

As mentioned above, the spin-crossover temperature is defined as the temperature at which the populations of the low- and high-spin states are equal. Because of this, $T_{1/2}$ is the target property in the development of SC systems for technological applications at room temperature. Experimentally, $T_{1/2}$ is generally determined through the analysis of the magnetic moments and Mössbauer spectra measured as a function of temperature.[1,70,71] From a thermodynamic point of view, the spin crossover can be described as an equilibrium between the low- and high-spin states for which the corresponding free energy is[72,73]

dx.doi.org/10.1021/ic300750c | Inorg. Chem. 2012, 51, 8194−8201

$$\Delta G = G^{HS}(T) - G^{LS}(T) \quad (1)$$

where

$$G^{i}(T) = H^{i} - TS = E^{i}_{el} + E^{i}_{vib} - TS \quad (2)$$

In eq 2, the enthalpy term contains both the electronic (E_{el}) and vibrational (E_{vib}) contributions. The latter can be obtained, with good accuracy, within the harmonic approximation. The electronic term (E_{el}) can be directly obtained from DFT calculations, although its value can vary significantly depending on the functional.

Since, at equilibrium, the free energy change ΔG must vanish, eq 1 can be used to calculate the spin-crossover temperature as

$$T_{1/2} = \frac{\Delta H}{\Delta S} \quad (3)$$

where the enthalpy and entropy changes are evaluated within the harmonic approximation. The equilibrium condition between the populations of the LS and HS states can also be expressed in terms of the corresponding equilibrium constant, K_{eq}, as

$$\Delta G(T) = -RT \ln K_{eq} = -RT \ln \frac{\gamma_{HS}}{1 - \gamma_{HS}} \quad (4)$$

where γ_{HS} is the relative population of the high-spin species. Therefore, eqs 1−4 can be used to calculate the relative population of the HS species as a function of the temperature, which, in turn, enables the calculation of the corresponding magnetic moment within the spin only approximation.[74] It is important to note that, although eqs 1−4 allow for an accurate calculation of the spin-crossover temperature, the overall shape of the variation of the magnetic moment obtained from measurements on the actual bulk material may not be well reproduced. This is mainly due to fact that cooperative effects present in the bulk material are missing in the calculations performed on the isolated molecular complex. In this regard, more sophisticated computational approaches have been proposed which account for the interaction between neighbor metal centers.[72,75] In some cases, these models have been successful in reproducing the variation of the magnetic moment of SC systems, although not all of the experimental data could be reproduced satisfactorily.[72]

3. RESULTS

3.1. Geometries of Spin-Crossover Complexes. The available experimental data show that the spin crossover in LD-LISC compounds is accompanied by significant changes in the bonding distances between the metal center and the ligands.[1] This can be directly related to the differences in the underlying electronic structure of the two spin states that arise from the different occupation of the non-bonding and antibonding molecular orbitals. In the case of Fe(II) centers in a six-coordinated octahedral environment, the low-spin state corresponds to a configuration in which the metal d electrons occupy the nonbonding t_{2g} set. By contrast, in the high-spin state, the metal d electrons also occupy the antibonding e_g orbitals, which leads to an increase in the metal-ligand distances with respect to the low-spin state.

Previous studies have shown that DFT methods can reproduce molecular geometries quite accurately independently of the specific functional used in the calculations.[42,76,77] A comparison of the calculated Fe−N distances (for both the axial and equatorial ligands) and coordination angles with the corresponding crystallographic data[26] available for the [Fe(stpy)$_4$(NCSe)$_2$] complex in the low-spin state is reported in Table 1. All functionals considered in this study are capable of reproducing the crystallographic parameters, with the TPSSh functional displaying the best agreement with the experimental values. Importantly, all functionals correctly reproduce the expansion of the bond distances upon the spin transition

Table 1. Comparison of the Average Calculated Values for the Bond Distances and Angles of the [Fe(stpy)$_4$(NCSe)$_2$] Complex with the Corresponding Crystallographic Data[26]

low-spin	d(Fe−N)$_{ax}$/Å	d(Fe−N)$_{eq}$/Å	angle/deg
B3LYP(*)	1.96	2.04	90.0
OLYP	1.93	2.03	90.0
OPBE	1.90	1.99	90.0
TPSSh	1.93	2.00	90.0
Crystal	1.94	2.00	90.0
high-spin	d(Fe−N)$_{ax}$/Å	d(Fe−N)$_{eq}$/Å	angle/deg
B3LYP(*)	2.09	2.28	90.0
OLYP	2.05	2.34	90.0
OPBE	2.04	2.30	90.0
TPSSh	2.07	2.24	90.0
Crystal	2.12	2.22	90.0

(Table 2). The optimized structures of the *trans*-[Fe(stpy)$_4$(NCSe)$_2$] complex in both spin states calculated with

Table 2. Comparison of the Calculated Changes in the Bond Distances for the [Fe(stpy)$_4$(NCSe)$_2$] Molecule Relative to the Crystallographic Data[26]

functional	Δd(Fe−N)$_{ax}$/Å	Δd(Fe−N)$_{eq}$/Å
B3LYP(*)	0.13	0.25
OLYP	0.12	0.31
OPBE	0.14	0.31
TPSSh	0.14	0.24
Crystal	0.18	0.22

the TPSSh functional are superimposed with the corresponding crystallographic data in Figure 2. The bond distances and angles of the first coordination sphere as well as the relative orientations of the pyridine rings are well reproduced. As discussed below, this is key to the correct description of the electronic structure of both spin states, which results in an accurate estimate of the electronic energy difference. Similar agreement between the crystallographic and calculated structural parameters is also obtained for the [Fe(stpy)$_4$(NCS)$_2$] complex in the high-spin state (see the Supporting Information). In all cases, the unrestricted high-spin calculations indicate a negligible degree of spin contamination. The $\langle S^2 \rangle$ value obtained with the TPSSh functional is equal to 6.08, 6.07, and 6.05 for the complex with the NCS, NCSe, and NCBH$_3$ ligands, respectively, which has to be compared with the ideal value of 6.00 for the pure spin state. Importantly, the unrestricted calculations for the low-spin state provide identical results to those obtained using the spin-restricted framework. This strongly suggests that the LD-LISC complexes considered in this study can be accurately described by a single determinant in both the high- and low-spin states.

3.2. Electronic Energies and Spin-Crossover Temperatures. The energy differences calculated for the three *trans*-[Fe(stpy)$_4$(NCX)$_2$] complexes are reported in Table 3. Among the functionals considered in this study, only TPSSh correctly predicts the low-spin state ($S = 0$) to be the ground state. This indicates that, due to the overstabilization of the high-spin state, the OLYP, OPBE, and B3LYP(*) functionals are not capable of reproducing the spin-crossover behavior of the LD-LISC complexes examined here. To estimate the free energy change associated with the conversion between the low- and high-spin states, the thermochemistry analysis was carried out for all three

dx.doi.org/10.1021/ic300750c | Inorg. Chem. 2012, 51, 8194−8201

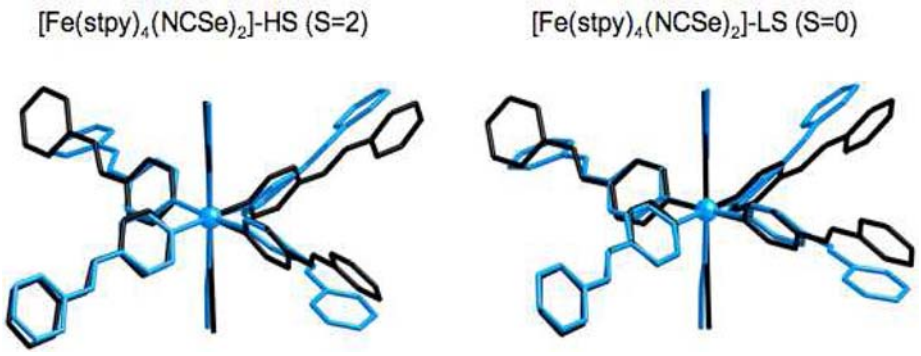

Figure 2. Overlap of the crystallographic (black) and calculated (blue) structures for the $[Fe(stpy)_4(NCSe)_2]$ in both spin states (left, high-spin; right, low-spin). The hydrogen atoms are omitted for clarity.

Table 3. Electronic Energies (in kcal/mol) of the High-Spin and Low-Spin States for the $[Fe(stpy)_4(NCX)_2]$ Complexes (X = S, Se, and BH_3)[a]

	$[Fe(stpy)_4(NCS)_2]$-HS	$[Fe(stpy)_4(NCS)_2]$-LS
OLYP	0.00	10.16
OPBE	0.00	5.11
B3LYP(*)	0.00	1.28
TPSSh	6.55	0.00
	$[Fe(stpy)_4(NCSe)_2]$-HS	$[Fe(stpy)_4(NCSe)_2]$-LS
OLYP	0.00	8.95
OPBE	0.00	3.92
B3LYP(*)	0.10	0.00
TPSSh	7.97	0.00
	$[Fe(stpy)_4(NCBH_3)_2]$-HS	$[Fe(stpy)_4(NCBH_3)_2]$-LS
OLYP	0.00	3.39
OPBE	2.02	0.00
B3LYP(*)	3.27	0.00
TPSSh	11.29	0.00

[a]Zero is assigned to the ground state.

$[Fe(stpy)_4(NCX)_2]$ complexes within the harmonic approximation. Equation 3 was then used to calculate the corresponding spin-crossover temperatures that are compared in Figure 3 with the available experimental data. Although the calculated values are ~57 K higher than the experimental data, the change of $T_{1/2}$ associated with the substitution of S by Se and BH_3 is correctly reproduced (Table 4), which is consistent with the isostructural character of $[Fe(stpy)_4(NCX)_2]$ with X = S and Se. This implies that the TPSSh functional is capable of describing the variation of the electronic structure of the $[Fe(stpy)_4(NCX)_2]$ complexes due to the chemical modification of the axial ligands. It is important to mention that no crystal structure is currently available for $[Fe(stpy)_4(NCBH_3)_2]$, and a slightly lower $T_{1/2}$ for this complex was reported in ref 25. The results of Figure 3 thus indicate that the TPSSh functional can effectively be used to predict both the structural parameters and spin-crossover temperatures of the LD-LISC complexes. Also shown in Figure 3 are the magnetic moments of each complex calculated as a function of the

Table 4. Experimental and Calculated (with the TPSSh Functional) Spin-Crossover Temperatures ($T_{1/2}$) for the $[Fe(stpy)_4(NCX)_2]$ Complexes (X = S, Se, BH_3)[a]

	$T_{1/2}$ (exptl.)	$T_{1/2}$ (calcd.)	ΔT
$[Fe(stpy)_4(NCS)_2]$	109[24]	159	50
$[Fe(stpy)_4(NCSe)_2]$	163[26]	214	51
$[Fe(stpy)_4(NCBH_3)_2]$	240[84]	309	69

[a]ΔT is the difference between the calculated and experimental values. All temperatures in K.

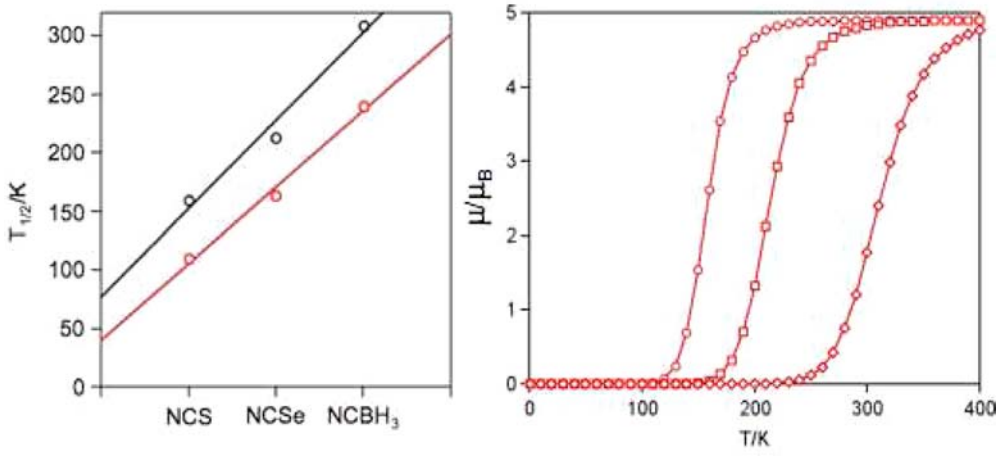

Figure 3. Left: Comparison of the experimental (red) and calculated (black) spin-crossover temperatures for the $[Fe(stpy)_4(NCX)_2]$ complexes (X = S, Se, and BH_3). Right: Calculated magnetic moments for the $[Fe(stpy)_4(NCX)_2]$ complexes with X = S (circle), Se (square), and BH_3 (diamonds) as a function of the temperature. See section 2 for computational details.

dx.doi.org/10.1021/ic300750c | Inorg. Chem. 2012, 51, 8194−8201

temperature. As mentioned above, since the isolated molecular models used in the calculations are not capable of recovering the cooperative effects present in the bulk material, the curves corresponding to the different complexes display essentially the same temperature dependence. In addition, the effects of intermolecular interactions and molecular-packing are not taken into account in the present model, which may be a source of discrepancy between the experimental and calculated values.

Another possible cause for the systematic overestimation of the spin-crossover temperature can also be related to the nature of the TPSSh functional. The parametrization of the TPSSh functional was performed by minimizing the mean absolute deviation of the enthalpies of formation for molecules in the G3/99 set,[78] which does not contain any transition metal complexes. Therefore, although the performance of the TPSSh functional in reproducing the spin-crossover behavior of the $[Fe(stpy)_4(NCX)_2]$ complexes is quite remarkable, it is likely that better agreement with the experimental data could be obtained after a specific reparameterization of the functional using a larger set of molecules including both transition metal and spin-crossover complexes.

3.3. Molecular Orbital Analysis. Fundamental insights into the spin-crossover behavior of the $[Fe(stpy)_4(NCX)_2]$ complexes can be gained from the analysis of the relevant molecular orbitals. In particular, the variation of $T_{1/2}$ observed with different NCX axial ligands can be directly related to the amount of π-backbonding of the axial ligands into the d_{xz} and d_{yz} metal d orbitals. In a perfect octahedral coordination environment (O_h), the d orbitals split in the well-known two over three orbitals scheme corresponding to the t_{2g} nonbonding and e_g antibonding sets of orbitals. When the symmetry of the complex is lowered to D_{4h} due to the presence of different ligands in the equatorial and axial positions, an additional splitting of the d-based molecular orbitals is observed. In the new point group, the d_{xz} and d_{yz} orbitals are expected to lie above the d_{xy} orbital due to the compression of the axial ligands in the low-spin state. The different ability of the axial ligands for π-backbonding then becomes the key factor in determining the ligand-field energy gap between the occupied and empty d-based MOs in the low-spin state (Δ), which is directly related to the spin-crossover temperature (Figure 4). It is important to mention that, although the symmetry of the studied systems is not exactly D_{4h}, the assumption of a perfect D_{4h} symmetry allows for a more direct analysis of the results in terms of the d-based molecular orbitals. Considering that all three $[Fe(stpy)_4(NCX)_2]$ complexes analyzed in the present study share the same equatorial ligand (stpy), minor changes of the d_{xy} (non-bonding) and $d_{x^2-y^2}$ (antibonding) orbitals are expected. Similarly, the d_{z^2} orbital, which is involved in a σ-antibonding interaction with the CN group, is expected to remain unaltered upon replacing S with Se and BH_3. Therefore, any change in the ligand field can be effectively attributed to the interaction of the axial ligands with the d_{xz} and d_{yz} orbitals. A more efficient π-backbonding ligand is expected to raise the energy of the d_{xz} and d_{yz} orbitals. This decreases the ligand field energy gap between the formerly nonbonding (d_{xz} and d_{yz}) and antibonding ($d_{x^2-y^2}$ and d_{z^2}) orbitals and, consequently, leads to a lower spin-crossover temperature. On the other hand, a poor π-backbonding ligand leaves the d_{xz} and d_{yz} orbitals almost unaltered, which results in a larger Δ and higher spin-crossover temperature. As shown in Figure 4, both the NCS and NCSe ligands have occupied π-type orbitals that interact with the d_{xz} and d_{yz} orbitals to form bonding and antibonding combinations. The stronger π-backbonding character of the NCS ligand is reflected in a larger energy difference between the bonding and antibonding combination with the d_{xz} and d_{yz} orbitals, which makes Δ for NCS smaller than for NCSe. On the other hand, being a very poor π-backbonding ligand, $NCBH_3$ leaves the non-bonding character of the d_{xz} and d_{yz} orbitals effectively unaltered upon coordination, which results in a larger Δ. All functionals used in this study provide ligand field energy gaps between the occupied and empty orbitals in the low-spin state in agreement with the qualitative diagram shown in Figure 4. In all cases, the energy difference between the bonding and antibonding combination is larger for NCS than NCSe. As expected, the Mulliken population analysis shows that the d-based molecular orbitals of the complex with NCSe have less d character due to the weaker π-backbonding character of the ligands (Table 5). The d_{xz} orbitals for the three $[Fe(stpy)_4(NCX)_2]$ complexes calculated with the TPSSh functional are shown in Figure 5. Analogous results (not shown) were obtained for the d_{yz} orbitals. The results clearly indicate the reduction of the d character of the d_{xz} orbital in the $[Fe(stpy)_4(NCSe)_2]$ complex due to weaker π-backbonding interactions (the d-character contribution to the d_{xz} orbital is 42.4%, 36.9%, and 53.4% for NCS, NCSe, and $NCBH_3$, respectively). Due to the absence of π-backbonding, both the

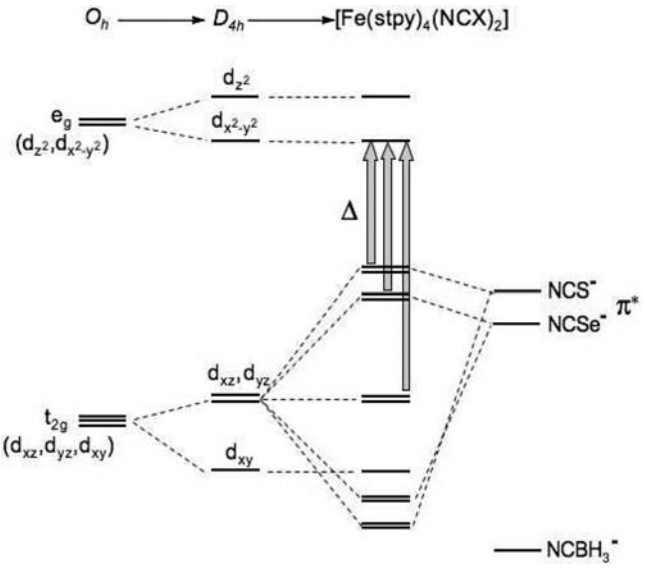

Figure 4. Schematic representation of the effects of the π-backbonding ability of the different axial ligands on the ligand-field energy gap between the occupied and empty d-based MOs in the low-spin state (Δ) in the $[Fe(stpy)_4(NCX)_2]$ (X = S, Se, and BH_3) family.

Table 5. Energy Differences (in cm^{-1}) between the Bonding and Antibonding Combinations of the d_{xz} and d_{yz} Pair of Orbitals with the p Orbitals of the NCX (X = S, Se) Ligand As Well As the Amount (%) of d Character of the Corresponding Molecular Orbital

	TPSSh	B3LYP(*)	OLYP	OPBE
ΔE(NCS)	10056	9663	9981	10781
d character	42.4	40.4	44.2	43.8
ΔE(NCSe)	9119	9411	8428	8618
d character	36.9	34.0	39.5	40.4

dx.doi.org/10.1021/ic300750c | Inorg. Chem. 2012, 51, 8194−8201

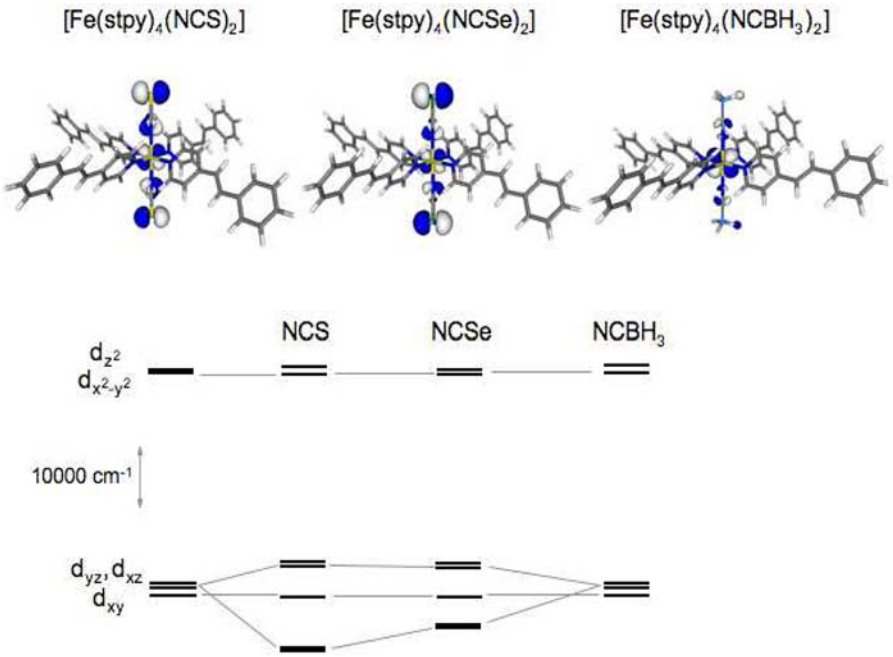

Figure 5. Molecular orbitals diagram for the $Fe(stpy)_4(NCX)_2]$ complexes (X = S, Se, BH_3) showing the d_{xz} orbital (0.04 $au^{-3/2}$ isovalue contour). The different π-backbonding ability of the axial ligand leads to different splittings of the d_{xz} and d_{yz} orbitals, which, in turn, modifies the ligand field and the spin-crossover temperature.

d_{xz} and d_{yz} orbitals of the $[Fe(stpy)_4(NCSe)_2]$ complex are effectively non-bonding, in agreement with the model predictions discussed above.

To directly correlate the picture that emerges from the analysis of the molecular orbitals with the corresponding spin-crossover temperature of the three $[Fe(stpy)_4(NCX)_2]$ complexes, time-dependent density functional theory (TD-DFT)[79−81] calculations were performed on the low-spin optimized molecules. It is well-known that, although DFT methods provide relatively accurate energy gaps, more reliable energies can be obtained using TD-DFT, which accounts for electron relaxation.[82] Using group theory arguments,[83] the transition energy calculated for the first d−d transition $^1A_{1g} \rightarrow {}^1E_g$ in the D_{4h} symmetry is 10 681, 11 002, and 12 028 cm^{-1} for the complexes with NCS, NCSe, and $NCBH_3$, respectively. These results clearly indicate that larger energy gaps arise when the S atom of the NCS ligand is replaced by Se and BH_3. This directly correlates with the calculated increase of the corresponding spin-crossover temperatures, which effectively measure the energy required to overcome the larger ligand fields generated by the axial ligands.

It is interesting to note that both spin states directly affect the splitting of the d-based molecular orbitals due to the different occupation of nonbonding and antibonding orbitals. In particular, shorter axial bonds are found in the low-spin state of all three $[Fe(stpy)_4(NCX)_2]$ complexes, which explains why the d_{z^2} orbital is higher in energy than the $d_{x^2-y^2}$ orbital, as well as why the d_{xz} and d_{yz} orbitals lie above the d_{xy} orbital. By contrast, in the high-spin state, the antibonding contribution arising from the axial ligand relaxes due to the larger bonding distances and energy splitting of each subset.

4. CONCLUSIONS

Spin-crossover complexes have recently attracted much interest due to their potential applications in the next generation of nanodevices, molecular sensors, and molecular memory systems. In this regard, ligand-driven light-induced spin change complexes represent a promising family of SC systems where the spin transition can be modulated by electromagnetic radiation. In this study we have presented a systematic analysis of the spin-crossover behavior of LD-LISC complexes belonging to the *trans*-$[Fe(stpy)_4(NCX)_2]$ family with X = S, Se, and BH_3. Specifically, four different DFT functionals (B3LYP(*), OLYP, OPBE, and TPSSh) have been used to calculate the spin-state energy differences as well as the underlying electronic structure. Among the four functionals, the present results indicate that TPSSh is the only functional capable of reproducing the correct ground state of the three LD-LISC complexes examined in this study. In particular, the TPSSh calculations provide accurate spin-crossover temperatures and, importantly, predict the correct dependence of $T_{1/2}$ on the chemical properties of the NCX axial ligands. The comparison with the corresponding experimental data indicates that the mean average error associated with the calculated $T_{1/2}$ is ∼58.5 K (0.11 kcal/mol). The TPSSh functional also provides structural properties for the three LD-LISC complexes in good agreement with the available crystallographic values. The direct analysis of the underlying electronic structure based on the calculated molecular orbitals provides fundamental insights into the dependence of $T_{1/2}$ on the nature of the axial ligands, which is explained in terms of the different π-backbonding ability of NCS, NCSe, and $NCBH_3$. Interestingly, it has recently been proposed that the incorporation of LD-LISC units into metal−organic frameworks could lead to the development of multifunctional materials in which the spin-crossover properties can be directly modulated through the adsorption of guest molecules as well as by chemical modifications of the ligands. In this context, the present calculations suggest that the TPSSh functional could eventually be used in hybrid quantum-mechanics/molecular-mechanics approaches aimed at the characterization of the spin-crossover behavior of MOF materials.

dx.doi.org/10.1021/ic300750c | *Inorg. Chem.* 2012, 51, 8194−8201

■ ASSOCIATED CONTENT

Supporting Information

Cartesian coordinates for all optimized structures of the $[Fe(stpy)_4(NCX)_2]$ complexes obtained with the TPSSh functional along with the corresponding energies and fitting parameters in eq 4. A comparison between the calculated and crystallographic structure of $[Fe(stpy)_4(NCS)_2]$ in the high-spin ($S = 2$) state is also shown. This material is available free of charge via the Internet at http://pubs.acs.org.

■ AUTHOR INFORMATION

Corresponding Author

*E-mail: fpaesani@ucsd.edu.

Notes

The authors declare no competing financial interest.

■ ACKNOWLEDGMENTS

This research was supported by start-up funds from the University of California at San Diego. We are grateful to the San Diego Supercomputer Center for a generous allocation of computer time on the Triton Computing Cluster.

■ REFERENCES

(1) Gütlich, P.; Goodwin, H. A. *Top. Curr. Chem.*: Springer: New York, 2004; Vol. *233*−*235*.
(2) Goodwin, H. A. *Coord. Chem. Rev.* **1976**, *18*, 293.
(3) Gütlich, P. *Struct. Bonding (Berlin)* **1981**, *44*, 83.
(4) Toftlund, H. *Coord. Chem. Rev.* **1989**, *94*, 67.
(5) König, E. *Struct. Bonding (Berlin)* **1991**, *76*, 51.
(6) Bousseksou, A.; Molnar, G.; Salmon, L.; Nicolazzi, W. *Chem. Soc. Rev.* **2011**, *40*, 3313.
(7) Halcrow, M. A. *Chem. Soc. Rev.* **2011**, *40*, 4119.
(8) Nihei, M.; Shiga, T.; Maeda, Y.; Oshio, H. *Coord. Chem. Rev.* **2007**, *251*, 2606.
(9) Cambi, L.; Szego, L. *Chem. Ber. Dtsch. Ges.* **1931**, *64*, 2591.
(10) Kahn, O.; Martinez, C. J. *Science* **1998**, *279*, 44.
(11) Bousseksou, A.; Molnar, G.; Matouzenko, G. *Eur. J. Inorg. Chem.* **2004**, *2004*, 4353.
(12) Salitros, I.; Madhu, N.; Boca, R.; Pavlik, J.; Ruben, M. *Monatsch. Chem.* **2009**, *140*, 695.
(13) Roques, N.; Mugnaini, V.; Veciana, J. In *Functional Metal-Organic Frameworks: Gas Storage, Separation and Catalysis*; Schroder, M., Ed.; Springer-Verlag Berlin: Berlin, Germany, 2010; Vol. *293*, p 207.
(14) Carne, A.; Carbonell, C.; Imaz, I.; Maspoch, D. *Chem. Soc. Rev.* **2011**, *40*, 291.
(15) Muñoz, M. C.; Real, J. A. *Coord. Chem. Rev.* **2011**, *255*, 2068.
(16) Gütlich, P.; Garcia, Y.; Goodwin, H. A. *Chem. Soc. Rev.* **2000**, *29*, 419.
(17) Real, J. A.; Gaspar, A. B.; Muñoz, M. C. *Dalton Trans.* **2005**, 2062.
(18) Thompson, A. L.; Money, V. A.; Goeta, A. E.; Howard, J. A. K. *C. R. Chim.* **2005**, *8*, 1365.
(19) Decurtins, S.; Gütlich, P.; Hasselbach, K. M.; Hauser, A.; Spiering, H. *Inorg. Chem.* **1985**, *24*, 2174.
(20) Decurtins, S.; Gütlich, P.; Köhler, C. P.; Spiering, H.; Hauser, A. *Chem. Phys. Lett.* **1984**, *105*, 1.
(21) Desaix, A.; Roubeau, O.; Jeftić, J.; Haasnoot, J. G.; Boukheddaden, K.; Codjovi, E.; Linares, J.; Nogues, M.; Varret, F. *Eur. Phys. B.* **1998**, *6*, 183.
(22) Jeftić, J.; Hinek, R.; Capelli, S. C.; Hauser, A. *Inorg. Chem.* **1997**, *36*, 3080.
(23) Renz, F.; Spiering, H.; Goodwin, H. A.; Gütlich, P. *Hyperfine Interact.* **2000**, *126*, 155.
(24) Roux, C.; Zarembowitch, J.; Gallois, B.; Granier, T.; Claude, R. *Inorg. Chem.* **1994**, *33*, 2273.
(25) Boillot, M.-L.; Roux, C.; Audière, J.-P.; Dausse, A.; Zarembowitch, J. *Inorg. Chem.* **1996**, *35*, 3975.
(26) Boillot, M.-L.; Pillet, S.; Tissot, A.; Rivière, E.; Claiser, N.; Lecomte, C. *Inorg. Chem.* **2009**, *48*, 4729.
(27) Boillot, M.-L.; Chantraine, S.; Zarembowitch, J.; Lallemand, J.-Y.; Prunet, J. *New J. Chem.* **1999**, *23*, 179.
(28) *Metal-Organic Frameworks*; John Wiley & Sons, Inc.: Hoboken, NJ, 2010.
(29) *Metal-Organic Frameworks*; Wiley-VCH Verlag & Co. KGaA: Weinheim, Germany, 2011.
(30) Halder, G.; Kepert, C. J.; Moubaraki, B.; Murray, K. S.; Cashion, J. D. *Science* **2002**, *298*, 1762.
(31) Neville, S. M.; Moubaraki, B.; Murray, K. S.; Kepert, C. J. *Angew. Chem., Int. Ed. Engl.* **2007**, *46*, 2059.
(32) Neville, S. M.; Halder, G.; Chapman, K. W.; Duriska, M. B.; Moubaraki, B.; Murray, K. S.; Cameron, J. K. *J. Am. Chem. Soc.* **2009**, *131*, 12106.
(33) Neville, S. M.; Halder, G.; Chapman, K. W.; Duriska, M. B.; Southon, D.; Cashion, J. D.; Létard, J.-F.; Moubaraki, B.; Murray, K. S.; Kepert, C. J. *J. Am. Chem. Soc.* **2008**, *130*, 2869.
(34) Halder, G. J.; Chapman, K. W.; Neville, S. M.; Moubaraki, B.; Murray, K. S.; Létard, J.-F.; Kepert, C. J. *J. Am. Chem. Soc.* **2008**, *130*, 17552.
(35) Geerlings, P.; De Proft, F.; Langenaeker, W. *Chem. Rev.* **2003**, *103*, 1793.
(36) Koch, W.; Holthausen, M. C. *A Chemist's Guide to Density Functional Theory*, Second ed.; Wiley-VCH: New York, 2001.
(37) Kohn, W.; Becke, A. D.; Parr, R. G. *J. Phys. Chem.* **1996**, *100*, 12974.
(38) Parr, R. G.; Yang, W. *Density-Functional Theory of Atoms and Molecules*; Oxford University Press: Oxford, U. K., 1989.
(39) Ziegler, T. *Chem. Rev.* **1991**, *91*, 651.
(40) Frenking, G.; Fröhlich, N. *Chem. Rev.* **2000**, *100*, 717.
(41) Siegbahn, P. E. M.; Blomberg, M. R. A. *Chem. Rev.* **2000**, *110*, 7040.
(42) Jensen, K. P.; Roos, B. O.; Ryde, U. *J. Chem. Phys.* **2007**, *126*, 014103.
(43) Paulsen, H.; Trautwein, A. X. *J. Phys. Chem. Solids* **2004**, *65*, 793.
(44) Paulsen, H.; Trautwein, A. X. *Top. Curr. Chem.* **2004**, *235*, 197.
(45) Reiher, M. *Inorg. Chem.* **2002**, *41*, 6928.
(46) Reiher, M. *Chimia* **2009**, *63*, 140.
(47) Reiher, M.; Salomon, O.; Hess, B. A. *Theor. Chem. Acc.* **2001**, *107*, 48.
(48) Swart, M.; Groenhof, A. R.; Ehlers, A. W.; Lammertsma, K. *J. Phys. Chem. A* **2004**, *108*, 5479.
(49) Staroverov, V. N.; Scuseria, G. E.; Tao, J.; Perdew, J. P. *J. Chem. Phys.* **2003**, *119*, 12129.
(50) Tao, J.; Perdew, J. P.; Staroverov, V. N.; Scuseria, G. E. *Phys. Rev. Lett.* **2003**, *91*, 146401.
(51) Jensen, K. P.; Cirera, J. *J. Phys. Chem. A* **2009**, *113*, 10033.
(52) Neese, F.; Wennmohs, F.; Hansen, A.; Becker, U. *Chem. Phys.* **2009**, *356*, 98.
(53) Rong, C.; Lian, S.; Yin, D.; Shen, B.; Zhong, A.; Bartolotti, L.; Liu, S. *J. Chem. Phys.* **2006**, *125*, 174102.
(54) Rong, C.; Lian, S.; Yin, D.; Zhong, A.; Zhang, R.; Liu, S. *Chem. Phys. Lett.* **2007**, *434*, 149.
(55) Jensen, K. P.; Ryde, U. *J. Phys. Chem. A* **2003**, *107*, 7539.
(56) Neese, F. *J. Biol. Inorg. Chem.* **2006**, *11*, 702.
(57) Zein, S.; Borshch, S. A.; Fleurat-Lessard, P.; E., C. M.; Chermette, H. *J. Chem. Phys.* **2007**, 14105.
(58) Daku, M. L.; Vargas, A.; Hauser, A.; Fouqueau, A.; Casida, M. E. *ChemPhysChem* **2005**, *6*, 1193.
(59) Hughes, T. F.; Friesner, R. A. *J. Chem. Theory. Comput.* **2011**, *7*, 19.
(60) Hughes, T. F.; Friesner, R. A. *J. Chem. Theory. Comput.* **2012**, *8*, 442.
(61) Becke, A. D. *J. Chem. Phys.* **1993**, *98*, 5648.
(62) Handy, N. C.; Cohen, A. J. *Mol. Phys.* **2001**, *99*, 403.

(63) Lee, C.; Yang, W.; Parr, R. G. *Phys. Rev. B: Condens. Matter* **1988**, *37*, 785.
(64) Perdew, J. P.; Burke, K.; Enzerhof, M. *Phys. Rev. Lett.* **1996**, *77*, 3865.
(65) Perdew, J. P.; Burke, K.; Ernzerhof, M. *Phys. Rev. Lett.* **1996**, 77.
(66) Staroverov, V. N.; Scuseria, G. E.; Tao, J.; Perdw, J. P. *J. Chem. Phys.* **2003**, *119*, 12129.
(67) Ye, S.; Neese, F. *Inorg. Chem.* **2010**, *49*, 772.
(68) Frisch, M. J.; Trucks, G. W.; Schlegel, H. B.; Scuseria, G. E.; Robb, M. A.; Cheeseman, J. R.; Scalmani, G.; Barone, V.; Mennucci, B.; Petersson, G. A.; Nakatsuji, H.; Caricato, M.; Li, X.; Hratchian, H. P.; Izmaylov, A. F.; Bloino, J.; Zheng, G.; Sonnenberg, J. L.; Hada, M.; Ehara, M.; Toyota, K.; Fukuda, R.; Hasegawa, J.; Ishida, M.; Nakajima, T.; Honda, Y.; Kitao, O.; Nakai, H.; Vreven, T.; Montgomery, J. A., Jr.; Peralta, J. E.; Ogliaro, F.; Bearpark, M.; Heyd, J. J.; Brothers, E.; Kudin, K. N.; Staroverov, V. N.; Kobayashi, R.; Normand, J.; Raghavachari, K.; Rendell, A.; Burant, J. C.; Iyengar, S. S.; Tomasi, J.; Cossi, M.; Rega, N.; Millam, N. J.; Klene, M.; Knox, J. E.; Cross, J. B.; Bakken, V.; Adamo, C.; Jaramillo, J.; Gomperts, R.; Stratmann, R. E.; Yazyev, O.; Austin, A. J.; Cammi, R.; Pomelli, C.; Ochterski, J. W.; Martin, R. L.; Morokuma, K.; Zakrzewski, V. G.; Voth, G. A.; Salvador, P.; Dannenberg, J. J.; Dapprich, S.; Daniels, A. D.; Farkas, Ö.; Foresman, J. B.; Ortiz, J. V.; Cioslowski, J.; Fox, D. J. *Gaussian 09*, Revision A.1; Gaussian, Inc.: Wallingford, CT, 2009.
(69) Schäfer, A.; Huber, C.; Ahlrichs, R. *J. Chem. Phys.* **1994**, *100*, 5829.
(70) Paulsen, H.; Schunermann, V.; Trautwein, A. X.; Winkler, H. *Coord. Chem. Rev.* **2005**, *249*, 255.
(71) Gütlich, P. *Z. Anorg. Allg. Chem.* **2012**, *638*, 15.
(72) Boča, R.; Linert, W. *Monatsch. Chem.* **2003**, *134*, 199.
(73) Gütlich, P.; Köppen, H.; Link, R.; Steinhäuser, H. G. *J. Chem. Phys.* **1979**, *70*, 3977.
(74) Kahn, O. *Molecular Magnetism*; VCH: New York, 1993; p 380.
(75) Spiering, H. *Top. Curr. Chem.* **2004**, *235*, 171.
(76) Furche, F.; Perdew, J. P. *J. Chem. Phys.* **2006**, *124*, 044103.
(77) Schultz, N. E.; Zhao, Y.; Truhlar, D. G. *J. Phys. Chem. A* **2005**, *109*, 11127.
(78) Curtiss, L. A.; Raghavachari, K.; Redfern, P. C.; Pople, J. A. *J. Chem. Phys.* **2000**, *112*, 7374.
(79) Bauernschmitt, R.; Ahlrichs, R. *Chem. Phys. Lett.* **1996**, *256*, 454.
(80) Casida, M. E.; Jamorski, C.; Casida, K. C.; Salahub, D. R. *J. Chem. Phys.* **1998**, *108*, 4439.
(81) Stratmann, R. E.; Scuseria, G. E. *J. Chem. Phys.* **1998**, *109*, 8218.
(82) Zhang, G.; Musgrave, C. B. *J. Phys. Chem. A* **2007**, *111*, 1554.
(83) Cotton, F. A. *Chemical Applications of Group Theory*, Third ed.; Wiley: New York, 1990.
(84) Sugahara, A.; Moriya, K.; Enomoto, M.; Okazawa, A.; Kojima, N. *Polyhedron* **2011**, *30*, 3127.